

---

# An improved hydrogen bond potential: Impact on medium resolution protein structures

---

FELCY FABIOLA,<sup>1</sup> RICHARD BERTRAM,<sup>1,2</sup> ANDREI KOROSTELEV,<sup>1,3</sup> AND MICHAEL S. CHAPMAN<sup>1,3</sup>

<sup>1</sup>Kasha Laboratory of Biophysics, Florida State University, Tallahassee, Florida 32306-4380, USA

<sup>2</sup>Department of Mathematics, Florida State University, Tallahassee, Florida 32306-4380, USA

<sup>3</sup>Department of Chemistry and Biochemistry, Florida State University, Tallahassee, Florida 32306-4380, USA

(RECEIVED December 11, 2001; FINAL REVISION March 5, 2002; ACCEPTED March 5, 2002)

## Abstract

A new semi-empirical force field has been developed to describe hydrogen-bonding interactions with a directional component. The hydrogen bond potential supports two alternative target angles, motivated by the observation that carbonyl hydrogen bond acceptor angles have a bimodal distribution. It has been implemented as a module for a macromolecular refinement package to be combined with other force field terms in the stereochemically restrained refinement of macromolecules. The parameters for the hydrogen bond potential were optimized to best fit crystallographic data from a number of protein structures. Refinement of medium-resolution structures with this additional restraint leads to improved structure, reducing both the free R-factor and over-fitting. However, the improvement is seen only when stringent hydrogen bond selection criteria are used. These findings highlight common misconceptions about hydrogen bonding in proteins, and provide explanations for why the explicit hydrogen bonding terms of some popular force field sets are often best switched off.

**Keywords:** Hydrogen bonds; crystallography; force field; hydrogen bond restraint

Force fields are critical to molecular simulation in many aspects of life sciences research. Understanding, analyzing, and predicting three-dimensional structural models of molecular systems—including their conformations, binding affinities, and related properties—all depend on accurate atomic force fields. For this reason, there has been a great deal of effort devoted to the development and improvement of potential energy functions and their parameterization.

The force fields commonly used for determining atom positions within a molecule use a combination of valence (or bonded) and nonbonded energy terms (Weiner and Kollman 1981; Brooks et al. 1983; Karplus 1987; Dinur and Hagler 1991). The overall potential energy of a molecular system may be written as

$$E_{\text{Empirical}} = E_{\text{bond}} + E_{\text{angle}} + E_{\text{dihedral}} + E_{\text{vdw}} + E_{\text{elec}} + E_{\text{hb}}$$

where the different energy terms are given by empirical formulae or harmonic functions penalizing deviations from ideal values. These values are determined from small-molecule crystallographic or spectroscopic data or from calibration to quantum mechanics calculations (Lifson and Stern 1982; Brooks et al. 1983; Nemethy et al. 1983; Hermans et al. 1984; Weiner et al. 1984, 1986; Nilsson and Karplus 1986; Dinur and Hagler 1991; Engh and Huber 1991). For macromolecular refinement with data from X-ray crystallography, an additional term is added,  $E_{\text{X-ray}}$ , which restrains the model against the diffraction data. The total potential energy is then

$$E_{\text{total}} = E_{\text{Empirical}} + w_a E_{\text{X-ray}}$$

where  $w_a$  is a weighting factor.

Energy minimizations and dynamics simulations are often limited by inadequate description of the various force

---

Reprint requests to: Michael S. Chapman, Kasha Laboratory of Biophysics, Florida State University, Tallahassee, FL 32306-4380, USA; e-mail: chapman@sb.fsu.edu; fax: (850) 644-7244.

Article and publication are at <http://www.proteinscience.org/cgi/doi/10.1110/ps.4890102>.

field parameters for the systems of interest. For example, if a crystallographically determined structure is energy minimized without structure factor penalty terms ( $E_{X\text{-ray}}$ ), then deviations from the experimental structure are often much larger (0.5 to 1.5 Å) than the expected error (Roberts et al. 1986), undermining confidence in molecular mechanics analyses. Here we focus on known shortcomings of explicit hydrogen bond force field terms that have led to their common omission from energy minimization (Brooks et al. 1983).

Hydrogen bonds are the key to many phenomena, including the formation and stabilization of secondary structures (Bordo and Argos 1994), protein folding and stability (Dill 1990; Fersht and Serrano 1993), molecular recognition (Fersht 1985), and drug binding and enzymatic reactions that involve transfer of protons (Cleland and Kreevoy 1994; Frey et al. 1994; Hutter and Helms 2000). Therefore, it is important that the geometry of hydrogen bonds be understood as completely as possible and incorporated into accurate potential functions. Appropriate restraining of hydrogen bonding interactions depends greatly on the selection criteria used to identify hydrogen bonds, and on the functional form of the potential describing the interactions.

The resolution of X-ray crystallography data for proteins rarely extends beyond 1.0 Å. For this reason, studies of hydrogen bonds in proteins have been mostly limited to the coordinates of nonhydrogen atoms, that is, donor-acceptor stereochemistry. Thus, the hydrogen bond selection criteria used in some of these studies are based on the distance between the potential donor and acceptor atoms (Ippolito et al. 1990; Mandel-Gutfreund et al. 1995). Other identification procedures use additional criteria for the angle made by donor, acceptor, and acceptor antecedent atoms (Stickle et al. 1992). However, the hydrogen bond geometry can be better understood in terms of the angle and distances involving the positions of hydrogen (Baker and Hubbard 1984), even if the hydrogen positions are modeled only implicitly from their heavy atom neighbors.

Several strategies have been used to account for hydrogen bonding in crystallographic refinement and molecular simulations. The hydrogen bond potential is often implicitly parameterized as a combination of Lennard-Jones (L-J) and electrostatic terms. In force fields that use an explicit hydrogen bonding term, the hydrogen bond potential is typically a distance-dependent function without any directional component. The functional form may be an L-J 6–12 type potential (Hagler et al. 1979; Jorgensen and Rives 1988; Cornell et al. 1995; MacKerell et al. 1998), an L-J 10–12 type (Momany et al. 1975; Brooks et al. 1983; Weiner et al. 1986), an L-J 6–9 type (Hagler et al. 1979; Ewig et al. 1999), or a Morse type potential (Hagler et al. 1974). A cosine directional term has been incorporated into CHARMM (Brooks et al. 1983), Dreiding II (Mayo et al. 1990), and MM3 (Lii and Allinger 1998). In these imple-

mentations, the hydrogen bond energy is minimized when the hydrogen bond N-H . . . O is linear, with an angle of 180°. However, these do not reflect the nonlinear directional preferences of hydrogen bonds at the acceptor that are conferred by their covalent component (Baker and Hubbard 1984; Gorbitz 1989; Ippolito et al. 1990; Stickle et al. 1992; Isaacs et al. 1999). Our goal was to develop a direction-dependent hydrogen bond function and appropriate selection criteria that improve crystallographic refinement. The hydrogen bond potential calibrated in this way by the crystallographic protein data would be optimized for protein environments, and could then possibly be used to better describe hydrogen bonds in molecular simulations or the refinement of other proteins.

Macromolecular structures are generally only determinable by combining experimental data with stereochemical restraints. Stereochemistry is especially important at lower resolutions, at which there is less data to define the atomic positions. The relative weighting of experimental data versus stereochemistry is usually determined empirically by cross-validation (Brünger 1997). Cross-validation involves the random selection of a proportion of the data (~10%) to be omitted from refinement. This data is used to compute a free R-factor ( $R^{\text{free}}$ ), an unbiased indicator of the quality of the refinement. Brünger (1997) suggested that an appropriate weight could be determined by trial and error, calculating  $R^{\text{free}}$  after separate refinements with an array of weights. The value of the weight giving the lowest  $R^{\text{free}}$  is thought to provide the best balance of experimental and stereochemical restraints. Here we extend this idea, using  $R^{\text{free}}$  to determine the most appropriate of several functional forms for a hydrogen bond restraint and to determine the most appropriate parameters.

## Results and Discussion

### *Improvement of structures using a main-chain hydrogen bond restraint*

A drop in  $R^{\text{free}}$  after refinement with a 10-protein training set (Table 1) shows the added hydrogen bonding restraint to be beneficial (Table 2). The drop in  $R^{\text{free}}$  varies from 0.6% to 1.8%, depending on the protein. This is a small numerical reduction, but large relative to the small increase in the number of stereochemical restraints. For CD2 and  $\beta$ -catenin, 150 and 460 hydrogen bond restraints are added, respectively, compared with the total number of other stereochemical restraints—11,176 and 14,417—for the two structures, respectively. An equivalent number of van der Waals interactions (150 and 460) affect  $R^{\text{free}}$  by only 0.07% and 0.03%, compared with 1.6% and 1.4% for the hydrogen bonds.

Another benefit of the hydrogen bonding restraint is that over-fitting is reduced (0.1% to 3.4%), as measured by the

**Table 1.** Protein structures used in the test refinements

PDB <sup>a</sup> code	Name	Resolution (Å)	Reported R <sup>free</sup>	Reported R	Reference
2CHR	chloromuconate cycloisomerase	3.0	26.4	18.9	Hoier et al. 1994
1A7B	CD2	3.1	30.6	23.9	Murray et al. 1998
2BCT	β-catenin	2.9	28.8	21.1	Huber et al. 1997
1A9B	complex (MHC-I/peptide)	3.2	30.5	25.1	Menssen et al. 1999
1A43	HIV-1 capsid protein	2.6	28.1	22.3	Worthylake et al. 1999
1AVC	bovine annexin VI	2.9	26.8	20.5	Avila-Sakar et al. 1998
6PFK	phosphofructokinase	2.6	25.5	18.8	Schirmer and Evans 1990
1AWU	cyclophilin A	2.34	35.1	31.6	Vajdos et al. 1997
1AS3	GDP-bound G42V mutant G1A1	2.4	27.4	21.2	Raw et al. 1997
1AB4	topoisomerase	2.8	31.0	22.6	Morais Cabral et al. 1997

<sup>a</sup> PDB, Protein Data Bank.

difference  $R^{\text{free}} - R$  (Kleywegt and Jones 1995; Kleywegt and Brünger 1996) or by the  $R^{\text{free}}/R$  ratio (Tickle et al. 1998a,b). As expected, refinement also improves the restrained geometry, both angles and distances, of the hydrogen bonds (Fig. 1).

It is medium-resolution structures that benefit most from the hydrogen bond restraints, because there is insufficient experimental data to determine unique atom positions without adding stereochemical restraints or constraints. High-resolution structures are not improved by the new restraints, but they should not be harmed. Refinement of a high-resolution (1.2 Å) arginine kinase transition state analog complex (M. Yousef, F. Fabiola, J. Gattis, T. Somasundaram, and M. Chapman, in prep.) with the hydrogen bond restraint improves  $R^{\text{free}}$  and decreases over-fitting, albeit only marginally ( $R^{\text{free}} = 17.79$  and  $R = 16.52$  with the restraint,

compared with  $R^{\text{free}} = 17.80$  and  $R = 16.45$  without). This shows that the hydrogen bonding restraint is not inconsistent with high-resolution crystallographic data. However, it also led us to the counter-intuitive choice of medium-resolution structures over high-resolution structures in the training set, because of the greater sensitivity of their refinements to the correct hydrogen bonding parameters.

Could the beneficial effects of an explicit hydrogen bond restraint be obtained implicitly through an electrostatic term? This was tested using the CNS program, in which introduction of electrostatics also required a change from the default repulsive function to a L-J 6–12 potential. The L-J/electrostatic combination yielded an  $R^{\text{free}}$  that was the same as for the repulsive treatment of contacts without a hydrogen bonding restraint. The addition of hydrogen bonding restraints, in both cases, lowered  $R^{\text{free}}$  by 0.6% to 1.8%. This shows that implicit electrostatic terms cannot replace explicit hydrogen bonding restraint.

To investigate the impact of the hydrogen bond restraint on poor models, it was included in the initial stages of refinement. With heavy weighting of the hydrogen bond restraint, the quality of refinement was reduced, likely caused by the trapping of the model in a local minimum of the potential energy function. It is recommended that hydrogen bond restraint be used only during the final stages of refinement.

#### Optimal parameters for the hydrogen bond potential

The parameters for the new restraint include the target donor-acceptor distance ( $R_0$ ), two target acceptor pseudo-bond angles ( $\theta_{\text{low}}$  and  $\theta_{\text{high}}$ ), and the strength or weight ( $\epsilon$ ) of a hydrogen bond relative to other stereochemical interactions. They also include cut-off criteria for the selection of hydrogen bonds:  $\theta_{\text{cut}}$  (the minimal  $\theta$ ) and  $R_{\text{cut}}$  (the maximum donor-acceptor distance). All parameters were initially optimized for each of the training proteins independently, and there is some variation (Table 3). There is little variation in

**Table 2.** Refinement statistics of test protein structures with and without the hydrogen bond restraint

PDB code	Refinement without a hydrogen-bond restraint <sup>a</sup>			Refinement with optimized hydrogen bond restraints <sup>b</sup>		
	R <sup>free</sup> (%)	R (%)	R <sup>free</sup> – R (%)	R <sup>free</sup> (%)	R (%)	R <sup>free</sup> – R (%)
2CHR	26.18	17.94	8.24	24.35	19.46	4.89
1A7B	31.64	22.85	8.79	29.06	23.98	5.08
2BCT	28.16	21.13	7.03	26.78	21.58	5.20
1A9B	30.69	25.57	5.12	29.83	25.44	4.39
1A43	27.72	22.07	5.65	26.77	21.93	4.84
1AVC	27.11	19.64	7.47	26.44	19.63	6.81
6PFK	24.02	16.78	7.24	23.54	16.93	6.61
1AWU	35.24	33.58	1.66	34.19	32.62	1.57
1AS3	27.18	21.86	5.32	26.67	21.76	4.91
1AB4	31.16	23.13	8.03	30.65	22.82	7.83

PDB, Protein Data Bank.

<sup>a</sup> R-factors are calculated in a consistent manner in this table and differ slightly from those of Table 1, which were calculated in the original structure determinations by the original authors using a variety of scaling procedures and refinement protocols.

<sup>b</sup> Hydrogen bond restraint parameters were optimized against each of these training proteins individually.

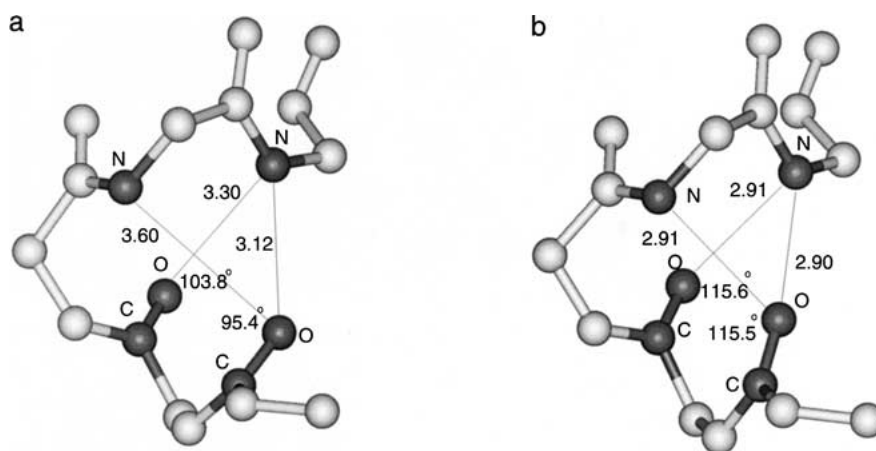


**Fig 1.** Main-chain hydrogen bond distances and angles are improved by refinement with the double-well hydrogen bond restraint. A region of chloromucanate cycloisomerase before refinement (*a*) and after refinement (*b*) with  $\varepsilon = 100$ . The atoms involved in hydrogen bonding interactions are shown in dark color. N...O distances and C = O...N angles are indicated.

the optimal target distance ( $R_0 = 2.9 \pm 0.1 \text{ \AA}$ ). The optimal angles ( $\theta_{\text{low}}$  and  $\theta_{\text{high}}$ ) lie in a narrow range ( $5^\circ$  to  $10^\circ$ ) for most of the proteins, with three exceptions. The optimal distance and angle cut values are similar for most proteins, with  $\theta_{\text{cut}} = 90^\circ$  and  $R_{\text{cut}} = 3.5 \text{ \AA}$  in most cases. These values are consistent with earlier protein database (Baker and Hubbard 1984) and quantum mechanical studies (Mitchell and Price 1990). The largest variation is in the optimal weight. The dependence of  $R^{\text{free}}$  on  $\varepsilon$  is shown in Figure 2 for three proteins. Even when a large value is optimal, all nonzero values lead to improvement, and most of the improvement comes with a modest value of  $\varepsilon$ . Higher values might be needed for some proteins if they contain regions of structure that need to be dislodged from an incorrect local energy minimum that does not have good hydrogen bonding configuration.

It would be desirable to have a single parameter set that can be applied in future refinements without further optimization. The consensus parameter set that was tested was  $\varepsilon = 100$ ,  $\theta_{\text{low}} = 115^\circ$ ,  $\theta_{\text{high}} = 155^\circ$ ,  $R_0 = 2.9 \text{ \AA}$ ,

$R_{\text{cut}} = 3.5 \text{ \AA}$ , and  $\theta_{\text{cut}} = 90^\circ$ . Refinement with this set improved all 10 training structures, although individual optimization of  $\varepsilon$  or all hydrogen bond parameters led to further improvement (Fig. 3). For future refinements, the consensus angular and distance parameters are likely adequate, but a one-dimensional search for optimal weight might be worthwhile.

For our high-resolution test case (arginine kinase), refinement with the consensus parameters slightly reduced  $R^{\text{free}}$  (0.01%). In contrast, refinement with a set of nonoptimal parameters (setting,  $\theta_{\text{low}} = 90^\circ$  and  $\theta_{\text{high}} = 155^\circ$ ) increased  $R^{\text{free}}$  by 0.3%. This shows that the optimal parameters obtained based on medium-resolution structures are consistent with those from a high-resolution structure.

Ramachandran plots (Ramakrishnan and Ramachandran 1965) of structures refined with the double-well hydrogen

**Table 3.** Optimal hydrogen bond parameters

Protein	$\varepsilon$	Optimal parameters				
		$R_0$ ( $\text{\AA}$ )	$\theta_{\text{low}}$ ( $^\circ$ )	$\theta_{\text{high}}$ ( $^\circ$ )	$R_{\text{cut}}$ ( $\text{\AA}$ )	$\theta_{\text{cut}}$ ( $^\circ$ )
2CHR	1500	2.9	115	169	3.4	90
1A7B	1600	2.8	115	155	3.5	90
2BCT	100	2.9	112	168	3.4	90
1A9B	300	2.9	115	155	3.5	95
1A43	99	2.9	115	149	3.5	90
1AVC	63	2.9	90	165	3.5	100
6PFK	161	2.9	115	155	3.5	90
1AWU	35	3.0	96	155	3.7	95
1AS3	49	2.9	100	163	3.5	90
1AB4	93	2.9	95	155	3.5	90

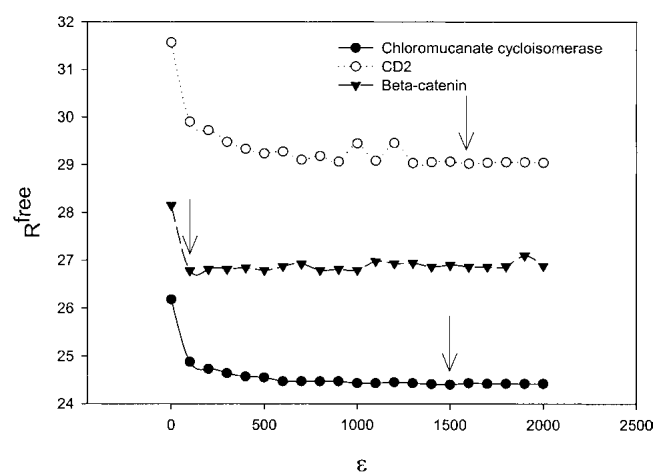


**Fig 2.** Free R-factor ( $R^{\text{free}}$ ) versus weight ( $\varepsilon$ ) for the main-chain hydrogen bond restraint. Each refinement was performed with optimized hydrogen bond parameters. Optimal  $\varepsilon$  are indicated by arrows.

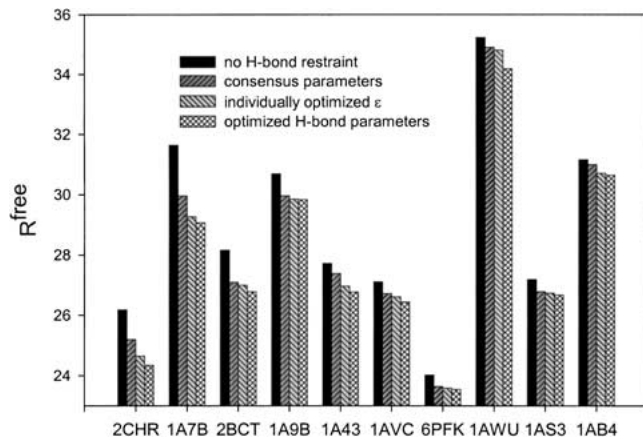


**Fig 3.** Results of refinements without the hydrogen bond restraint, or with the restraint and various parameter sets. The consensus parameters were  $\epsilon = 100$ ,  $\theta_{\text{low}} = 115^\circ$ ,  $\theta_{\text{high}} = 155^\circ$ ,  $R_{\text{cut}} = 3.5 \text{ \AA}$ ,  $\theta_{\text{cut}} = 90^\circ$ , and  $R_0 = 2.9 \text{ \AA}$ .

bond restraint show that good  $\phi$ ,  $\psi$  stereochemistry is retained. The root mean square difference values are marginally improved with structures refined with the hydrogen-bonding potential.

#### Hydrogen bond selection criteria

Our selection of hydrogen bonds was based on four criteria: (1) D...A distance  $< R_{\text{cut}}$ , (2) AA-A...D angle  $> \theta_{\text{cut}}$ , (3) H...A distance  $< 2.7 \text{ \AA}$ , and (4) D-H...A angle  $> 90^\circ$ . D indicates donor; A, acceptor; and AA, acceptor antecedent. Many force fields use just the first two criteria for selecting hydrogen bonds (Brooks et al. 1983; Ippolito et al. 1990; Mandel-Gutfreund et al. 1995). This has the advantage that explicit hydrogen positions are not required. The full set of four criteria resembles those of Baker and Hubbard (1984) and requires hydrogen positions to be predicted for those structures at resolutions insufficient to resolve them directly. In refinements reported here, hydrogen positions were predicted automatically by the refinement software.

Figure 4 shows  $R^{\text{free}}$  for refinements using the first two or all four hydrogen bond selection criteria. Refinements with four selection criteria are significantly better than those with two. With large weights, refinements with two criteria are inferior to those with no hydrogen bond restraint at all ( $\epsilon = 0$ ). The two selection criteria are insufficient to eliminate false-positive identifications, and restraining these false interactions distorts the refined structure. This emphasizes the importance of selection criteria that include the H...A distance and D-H...A angle. Indeed, it is likely that the primary factor in the failure of prior hydrogen bond restraints in some force field sets was insufficiently tight selection criteria.

#### Single- and double-well potentials

Figure 5 shows histograms of unrestrained C = O...N angles in three structures:  $\beta$ -catenin (2.9  $\text{\AA}$ ), CD2 (3.1  $\text{\AA}$ ) at medium resolution, and arginine kinase at high resolution (1.2  $\text{\AA}$ ). In all cases, the histograms show a bimodal acceptor angle distribution for peptide carbonyl oxygens. It is similar to the distribution seen in analysis of 42 protein structures (Stickle et al. 1992). Stickle et al. (1992) attributed the bimodality directly to different steric constraints for  $\alpha$ -helices versus  $\beta$ -sheets. However, our analysis and reexamination of the data presented by Stickle et al. shows that the bimodality extends to carbonyl groups that are neither  $\alpha$  nor  $\beta$ . Thus, the bimodality appears to be intrinsic to carbonyl oxygens, owing to both electrostatic and lone-pair covalent contributions to hydrogen bonds. The correlation of the peaks with  $\alpha$  and  $\beta$  structure, seen by both Stickle et al. (1992) and ourselves, is a secondary effect in which  $\alpha$  and  $\beta$  place different additional steric constraints, choosing differently between two intrinsically allowable carbonyl configurations.

It was shown by Bowie (1997) that a statistical bias exists in the distribution of an angle like the AA-A...D angle in three-dimensional space. Briefly, in a random angle distribution, the frequency of occurrence of angles  $\sim 180^\circ$  is much less than that of angles  $\sim 90^\circ$ . Following Bowie (1997), we have removed this bias by normalizing the AA-A...D angle distribution by the nonuniform random distribution. When normalized in this way, we still observe bimodal distributions, although now the rightmost peak is accentuated (Fig. 5, gray bars).

Figure 6 illustrates that refinement of chloromuconate cycloisomerase with a double-well hydrogen bond potential is superior to refinement with a single-well potential or a

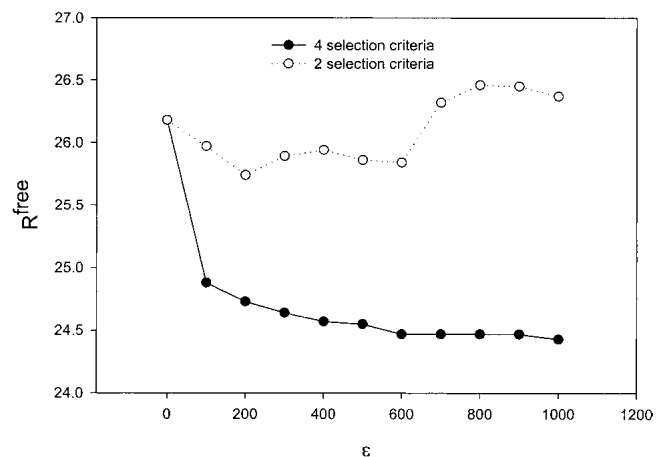


**Fig 4.** Free R-factor ( $R^{\text{free}}$ ) versus hydrogen-bond weight for chloromuconate cycloisomerase. Selection of hydrogen bonds is based on two or four criteria. Each refinement was performed with other hydrogen bond parameters fixed at consensus values.

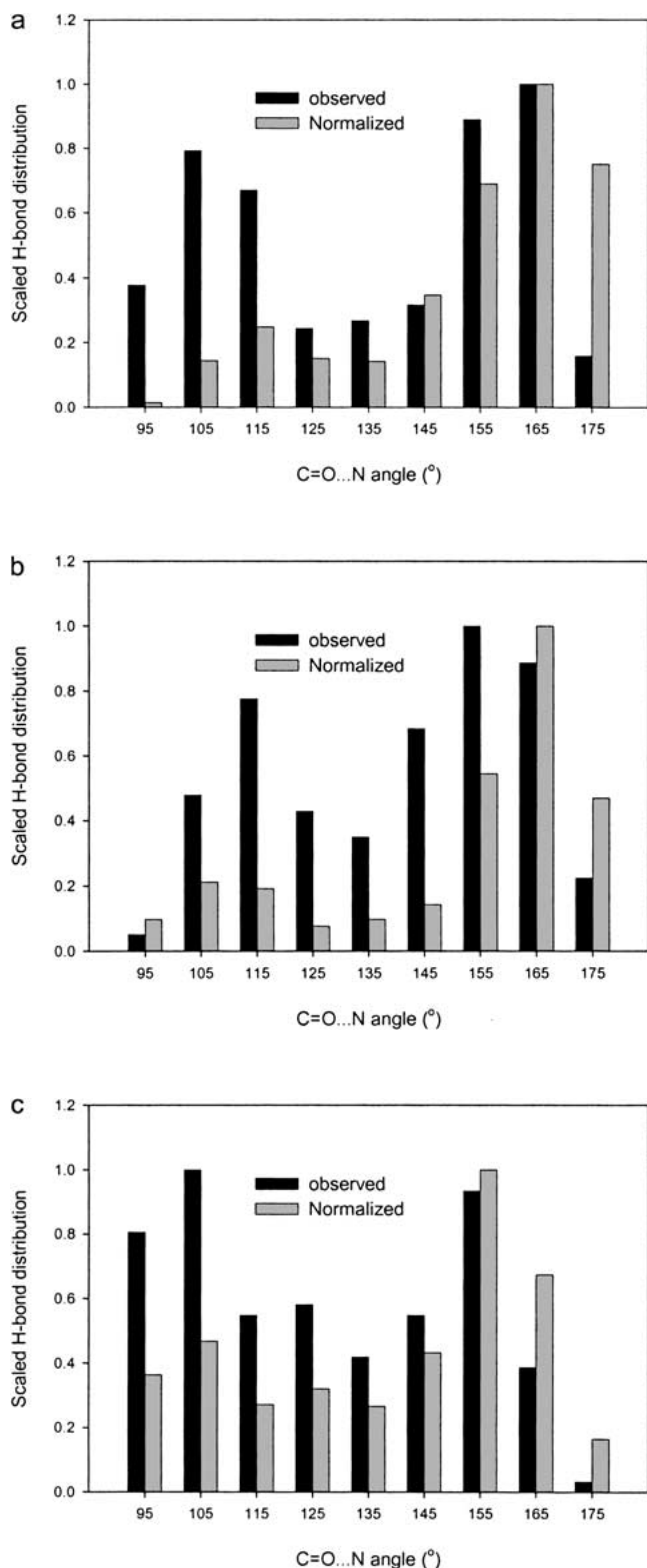


**Fig. 5.** Normalized distribution of C=O...N acceptor angles before inclusion of hydrogen bond restraints in  $\beta$ -catenin (*a*; at 2.9 Å resolution) and arginine kinase (*b*; at 1.2 Å resolution) and CD2 (*c*; at 3.1 Å resolution). The gray bars show the distribution normalized by the nonuniform random distribution (Bowie 1997).

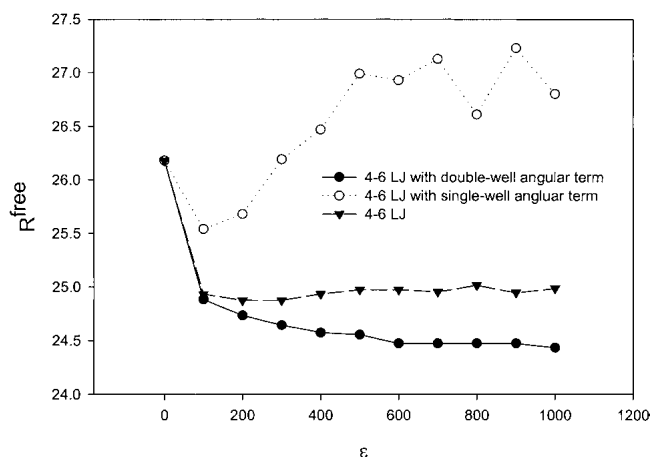


**Fig. 6.** Quality of refinements of chloromucanate cycloisomerase using double-well, single-well, and angle-independent hydrogen bond restraints. Consensus restraint parameters were used.

nondirectional L-J 4–6 potential. This is true for all training set proteins and is consistent with the observed bimodal angular distribution. Refinements with the nondirectional L-J 4–6 potential are superior to those with the single-direction L-J 4–6 potential, showing the importance of angular bimodality in the description of hydrogen bonds.

The improvements in refinement derive from both the new functional form and the stringent selection criteria. Comparison of Figures 4 and 6 reveals that the dominant factor is the selection criteria. The incorporation of a double-well angular component to the hydrogen bond potential gives additional improvement in  $R^{\text{free}}$  (Fig. 6), but only if four selection criteria are used.

Not surprisingly, refinement with the double-well hydrogen bond function redistributes C=O...N angles, producing larger peaks at the target angles and a reduction in the variance. This is illustrated in Figure 7 for refinement of chloromucanate cycloisomerase. Those angles initially greater than  $\theta_{\text{mid}} = 135^\circ$  are moved toward  $\theta_{\text{high}} = 155^\circ$ , and those initially less than  $\theta_{\text{mid}}$  are moved toward  $\theta_{\text{low}} = 115^\circ$ . The number of hydrogen bonds and their distribution at the end of the refinement depends on the weight ( $\epsilon$ ) given to the hydrogen bond potential.

#### Side-chain hydrogen bond restraint

The results presented thus far show that refinements of medium-resolution structures are improved with an appropriate main-chain hydrogen bond restraint. We now consider refinements with additional analogous side-chain hydrogen bond restraints. These additional hydrogen bonds could be side-chain to side-chain or side-chain to main-chain. The side-chains of Ser, Thr, and Tyr are involved in hydrogen bonding interactions through hydroxyl groups, Asp and Glu

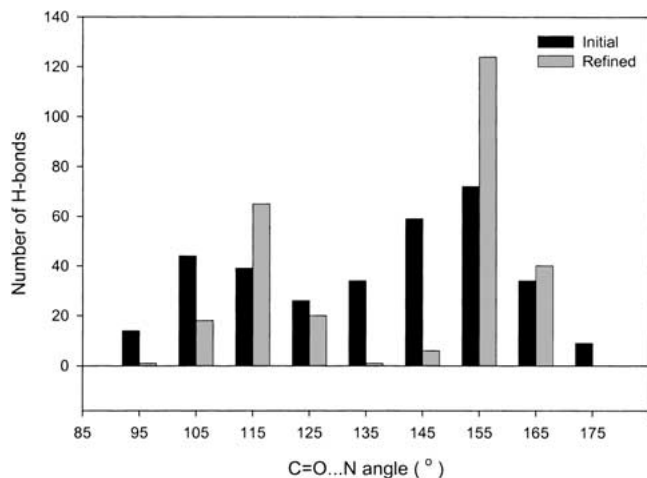


**Fig 7.** Distribution of C = O . . . N angles before and after refinement of chloromucanate cycloisomerase with the double-well hydrogen bond restraint ( $\epsilon = 100$ )

through carboxyl groups, Asn and Gln through carboximide groups, Lys through amino, Arg through guanidium, and His through imidazole groups. Although solvent water figures prominently in hydrogen bonding, the medium-resolution structures most improved by the new restraint had few water molecules explicitly modeled.

Parameters for the side-chain restraints were optimized as they had been for the main-chain. Refinements of the training set proteins with side-chain restraints but no main-chain restraints, reduces  $R^{\text{free}}$ . However, refinements with main-chain restraints alone are superior, and the best results are obtained when both main- and side-chain restraints are used. For example, refinements of chloromucanate cycloisomerase and HIV-capsid protein with main-chain restraints alone were improved by up to 0.5% when additional side-chain restraints were added (Fig. 8). The optimal target angle for the tetrahedral side-chain hydrogen bond acceptor was found to be  $109^\circ$ , consistent with expectations from stereochemistry.

In summary, this work shows that medium-resolution structures can be improved by an explicit hydrogen bond restraint. Improvement is possible only when stringent selection criteria are used that include explicit hydrogen positions. Angular terms for carbonyl oxygen acceptors help if they have a double-well form but are detrimental if unimodal. This indicates that force fields and energy minimizations that only consider the dipolar term and ignore covalent components are far from optimal.

## Materials and methods

### Hydrogen bond potential

The functional form of the hydrogen bond potential is as follows:

$$E_{\text{hb}} = \epsilon [(\sigma/R_{\text{D-A}})^6 - (\sigma/R_{\text{D-AA}})^4] \cos^4(\theta - \theta_0) \text{SW}(R_{\text{D-A}})$$

where  $\epsilon$  is a weight or strength of the hydrogen bond interaction;  $\sigma$  is related to the distance  $R_0$  at minimal potential,  $E_{\text{min}}$ , by  $\sigma = R_0\sqrt{2/3}$ ; and  $\theta$  and  $\theta_0$  are the D-A-AA and target D-A-AA angles, respectively. Thus, the hydrogen bond potential has both radial and angular parts. A switching function (Brunger 1992), SW, is applied to smoothly decrease  $E_{\text{hb}}$  to zero beyond a cut-off distance (Fig. 9a).

The “ideal” C = O . . . N angle at the acceptor oxygen has been a subject of debate (Donohue 1968), and the surveys based on small molecular structures (Mitra and Ramakrishnan 1977) show a wide range of values, between  $100^\circ$  and  $160^\circ$ . Our analysis of individual protein structures confirmed a bimodal acceptor C = O . . . N angle distribution (Fig. 5), as revealed by Stickle et al. (1992). This is incorporated within our force field term by substituting for  $\theta_0$  one of two target angles,  $\theta_{\text{low}}$  and  $\theta_{\text{high}}$ , whichever is closer to the current model  $\theta$ .  $\theta_{\text{low}}$  and  $\theta_{\text{high}}$  correspond to hydrogen bonds that are predominantly covalent and electrostatic, respectively. The angle dependence is illustrated in Figure 9b.

The hydrogen bond function was implemented as a module for the crystallographic refinement program CNS (Brünger et al. 1998), in which it adds to the default CNS restraints. The default CNS nonbonded repulsive function is replaced by the hydrogen bond function, when appropriate. Derivatives of the hydrogen bond energy are calculated and added to those calculated by CNS. Thus, all types of optimization performed by CNS, such as conjugate gradient minimization and simulated annealing, are supported with the additional restraint.

### Parameterization

Parameters were optimized with medium-resolution structures and their diffraction amplitudes, downloaded from the Protein Data Bank (PDB; Berman et al. 2000). The test reflections that we used to compute  $R^{\text{free}}$  were the same as those used in the original structure determinations.

Hydrogen bond geometry can be analyzed directly in terms of angle at the hydrogen, D-H . . . A, and the hydrogen bond distance, H . . . A, as well as indirectly with the angle D . . . A-AA and indirect distance D . . . A, as described in many force field sets

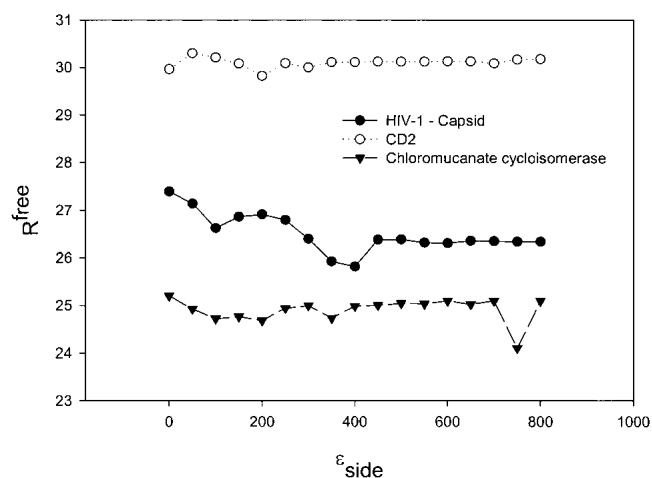


**Fig 8.** Refinement of three proteins as a function of the weight applied to side-chain hydrogen bond restraints. A weight of  $\epsilon_{\text{side}} = 0$  implies that no side-chain restraints were applied. Main-chain restraints were included in each case, with the consensus main-chain hydrogen bond parameters.

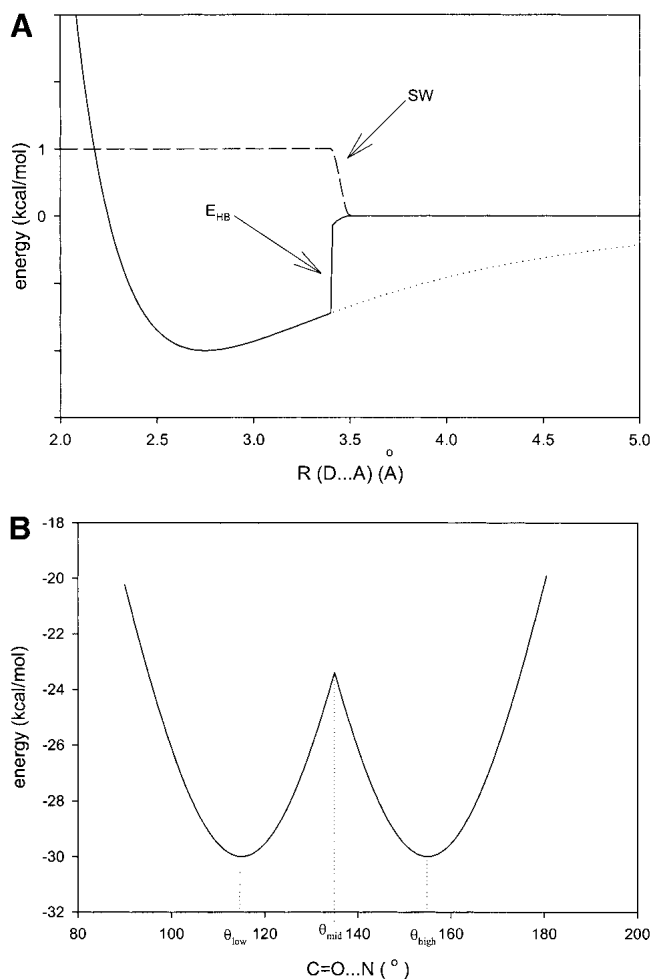


**Fig 9.** Hydrogen bonding restraining potential ( $E_{HB}$ ). (a) The radial component of the hydrogen bond potential with ( $E_{HB}$ , solid) and without (dotted) the switching function (SW). (b) The double-well angular component, for which  $\theta_{mid}$  is the midpoint between  $\theta_{low}$  and  $\theta_{high}$ .

(Baker and Hubbard 1984). However, hydrogen positions are required for direct analyses. Because medium-resolution X-ray structures typically do not include hydrogens, they were added at geometrically expected positions using CNS (Brünger et al. 1998). The occupancies of hydrogens were set to zero, so they would not contribute to calculated structure factor amplitudes, and any improvement in the refinement would be entirely owing to the improved stereochemical restraint.

Hydrogen bonding pairs were identified using the selection criteria of the form suggested by Baker and Hubbard (1984): (1)  $D \dots A$  distance  $< R_{cut}$ , (2)  $AA-A \dots D$  angle  $> \theta_{cut}$ , (3)  $H \dots A$  distance  $< 2.7 \text{ \AA}$ , and (4)  $D-H \dots A$  angle  $> 90^\circ$ .

Potential donor and acceptor pairs from within the same crystallographic asymmetric unit are identified according to these criteria by the new program module, and are updated on every refinement cycle. (Consideration of crystallographic symmetry and extension to nucleic acids are possible future enhancements.) Generous values of  $R_{cut}$  and  $\theta_{cut}$  were used to allow the refinement to improve initially poor hydrogen bond geometry. Control tests were performed with selection criteria 1 and 2 only.

The parameters  $\epsilon$ ,  $\theta_{low}$ ,  $\theta_{high}$ ,  $R_{cut}$ ,  $\theta_{cut}$ , and  $R_0$  were optimized by a grid search for the lowest  $R^{free}$  (Brünger, 1992). At each grid

point,  $R^{free}$  calculation followed reciprocal space conjugate gradient refinement. The first parameter to be optimized was  $\epsilon$ , using crude estimates for the other parameters.  $\epsilon$  values were obtained first for main-chain hydrogen bonds only. When side-chain hydrogen bonds were added, separate weights were found for main-chain and side-chain interactions. With optimal  $\epsilon$ , the target angles  $\theta_{low}$  and  $\theta_{high}$  were optimized, followed by the optimization of  $R_{cut}$ ,  $\theta_{cut}$ , and  $R_0$ . With optimal target angles and optimal  $R_{cut}$ ,  $\theta_{cut}$ , and  $R_0$  values, the weight  $\epsilon$  was again optimized.

Side-chain hydrogen bonds were classified into groups based on their geometries. Hydrogen bonds made by  $sp^2$  and  $sp^3$  hybridized acceptors have trigonal and tetrahedral geometries, respectively. The trigonal hydrogen bonds were restrained with a double-well potential, as were the main-chain hydrogen bonds. The tetrahedral hydrogen bonds were restrained with a single-well potential, because it is expected that the covalent component will dominate.

## Acknowledgments

We gratefully acknowledge the National Science Foundation (NSF) for support of methods development (NSF DBI 98-08098 to M.S.C.). R.B. was supported by NSF grants DBI 96-02233 and DMS 99-81822. We thank Mohammad Yousef, F.F., Jim Gattis, Thayumanaswamy Somasundaram, and M.S.C. for access to unpublished atomic coordinates of arginine kinase. Add-on software to implement the hydrogen bond potential in CNS will be made available at <http://www.sb.fsu.edu/~chapman>.

The publication costs of this article were defrayed in part by payment of page charges. This article must therefore be hereby marked "advertisement" in accordance with 18 USC section 1734 solely to indicate this fact.

## References

- Avila-Sakar, A.J., Creutz, C.E., and Kretsinger, R.H. 1998. Crystal structure of bovine annexin VI in a calcium-bound state. *Biochim. Biophys. Acta* **1387**: 103–116.
- Baker, E.N. and Hubbard, R.E. 1984. Hydrogen bonding in globular proteins. *Prog. Biophys. Mol. Biol.* **44**: 97–179.
- Berman, H.M., Westbrook, J., Feng, Z., Gilliland, G., Bhat, T.N., Weissig, H., Shindyalov, I.N., and Bourne, P.E. 2000. The Protein Data Bank. *Nucleic Acids Res.* **28**: 235–242.
- Bordo, D. and Argos, P. 1994. The role of side-chain hydrogen bonds in the formation and stabilization of secondary structure in soluble proteins. *J. Mol. Biol.* **243**: 504–519.
- Bowie, J.U. 1997. Helix packing angle preferences. *Nat. Struct. Biol.* **4**: 915–917.
- Brooks, B.R., Brucoleri, R.E., Olafson, B.D., States, D.J., Swaminathan, S., and Karplus, M. 1983. CHARMM: A program for macromolecular energy minimization, and dynamics calculations. *J. Comput. Chem.* **4**: 187–217.
- Brünger, A.T. 1992. *X-Plor Version 3.1. A system for crystallography and NMR*. Yale University Press, New Haven, CT.
- . 1992. Free R value: A novel statistical quantity for assessing the accuracy of crystal structures. *Nature* **355**: 472–475.
- . 1997. The free R value: A more objective statistic for crystallography. *Meth. Enzymol.* **277**: 366–396.
- Brünger, A.T., Adams, P.D., Clore, G.M., Gros, P., Gross-Kunstleve, R.W., Jiang, J.S., Kurzwski, J., Nilges, M., Pannu, N.S., Read, R.J., Rice, L.M., Simonson, T., and Warren, G.L. 1998. Crystallography and NMR system: A new software system for macromolecular structure determination. *Acta Cryst. D* **54**: 905–921.
- Cleland, W.W. and Kreevoy, M.M. 1994. Low-barrier hydrogen bonds and enzymic catalysis. *Science* **264**: 1887–1890.
- Cornell, W.D., Cieplak, P., Bayly, C.I., Gould, I.R., Merz, K.M.J., Ferguson, D.M., Spellmeyer, D.C., Fox, T., Caldwell, J.W., and Kollman, P.A. 1995. A second generation force field for the simulation of proteins, nucleic acids, and organic molecules. *J. Am. Chem. Soc.* **117**: 5179–5197.
- Dill, K.A. 1990. Dominant forces in protein folding. *Biochemistry* **29**: 7133–7155.



- Dinur, U. and Hagler, A.T. 1991. Approaches to empirical force fields. In *Review of computational chemistry*. (eds. K.B. Lipkowitz and D.B. Boyd), pp. 99–164. Wiley-VCH, New York, NY.
- Donohue, J. 1968. Selected topics in hydrogen bonding. In *Structural chemistry and molecular biology* (eds. W.H. Freeman, San Francisco. A. Rich and N. Davidson), pp. 443–465.
- Engh, R.A. and Huber, R. 1991. Accurate bond and angle parameters for X-ray protein structure refinement. *Acta Cryst. A* **47**: 392–400.
- Ewig, C.S., Thacher, T.S., and Hagler, A.T. 1999. Derivation of class II force fields, 7: Nonbonded force field parameters for organic compounds. *J. Phys. Chem. B* **33**: 6998–7014.
- Fersht, A. 1985. *Enzyme structure and function*, 2nd ed. Freeman, New York, NY.
- Fersht, A.R. and Serrano, L. 1993. Principles of protein stability from protein engineering experiments. *Curr. Opin. Struc. Biol.* **3**: 75–83.
- Frey, P.A., Whitt, S.A., and Tobin, J.B. 1994. A low-barrier hydrogen bond in the catalytic triad of serine proteases. *Science* **264**: 1927–1930.
- Gorbitz, C.H. 1989. Hydrogen-bond distances and angles in the structures of amino acids and peptides. *Acta Cryst. B* **45**: 390–395.
- Hagler, A.T., Huler, E., and Lifson, S. 1974. Energy functions for peptides and proteins, II: The amide hydrogen bond and calculation of amide crystal properties. *J. Am. Chem. Soc.* **96**: 5319–5327.
- Hagler, A.T., Lifson, S., and Dauber, P. 1979. Consistent force field studies of intermolecular forces in hydrogen bonded crystals, II: A benchmark for the objective comparison of alternative force fields. *J. Am. Chem. Soc.* **101**: 5122–5130.
- Hermans, Jr., J., Berendsen, W.F., van Gunsteren, W.F., and Postma, J.P.M. 1984. A consistent empirical potential for water-protein interactions. *Biopolymers* **23**: 1513–1518.
- Hoier, H., Schlomann, M., Hammer, A., Glusker, J.P., Carell, H.L., Goldman, A., Stezowski, J.J., and Heinemann, U. 1994. Crystal structure of chloromuconate cycloisomerase from *Alicyclobacillus eutrophus* JMP134 (PJP4) at 3 Å resolution. *Acta Cryst. D* **50**: 75–84.
- Huber, A.H., Nelson, W.J., and Weis, W.I. 1997. Three-dimensional structure of the armadillo repeat region of  $\beta$ -catenin. *Cell* **90**: 871–882.
- Hutter, M.C. and Helms, V. 2000. Phosphoryl transfer by a concerted reaction mechanism in UMP/CMP-kinase. *Protein Sci.* **9**: 2225–2231.
- Ippolito, J.A., Alexander, R.S., and Christianson, D.W. 1990. Hydrogen bond stereochemistry in protein structure and function. *J. Mol. Biol.* **215**: 457–471.
- Isaacs, E.D., Shukla, A., Platzman, P.M., Hamann, D.R., Barbiellini, B., and Tulk, C.A. 1999. Covalency of the hydrogen bond in ice: A direct X-ray measurement. *Phys. Rev. Lett.* **82**: 600–603.
- Jorgensen, W.L. and Rives, J.T. 1988. The OPLS (optimized potential for liquid simulations) potential functions for proteins, energy minimization for crystals of cyclic peptides and crambin. *J. Am. Chem. Soc.* **110**: 657–666.
- Karplus, M. 1987. The prediction and analysis of mutant structures. In *Protein engineering* (eds. D.L. Oxender and C.F. Fox), pp. 35–44. Alan R. Liss, New York, NY.
- Kleywegt, G.J. and Jones, T.A. 1995. Where freedom is given, liberties are taken. *Structure* **3**: 535–540.
- Kleywegt, G.J. and Brünger, A.T. 1996. Checking your imagination: Applications of the free R value. *Structure* **4**: 897–904.
- Lifson, S. and Stern, P. 1982. Born-Oppenheimer energy surfaces of similar molecules: Interrelations between bond lengths, bond angles, and frequencies of normal vibrations in alkanes. *J. Comput. Phys.* **77**: 4542–4550.
- Lii, J.-H. and Allinger, N.L. 1998. Directional hydrogen bonding in the MM3 force field: II. *J. Comput. Chem.* **19**: 1001–1016.
- MacKerell, A.D.J., Bashford, D., Bellott, M., Dunbrack, R.L.J., Evanseck, J.D., Field, M.J., Fisher, S., Gao, J., Guo, H., Ha, S., Joseph-McCarthy, D., Kuchnir, L., Kuczera, K., Lau, F.T.K., Mattos, C., Michnick, S.W., Ngo, S., Nguyen, D.T., Prodhom, B., Reiher III, W.E., Roux, B., Schlenkrich, M., Smith, J.C., Stote, R., Straub, J.E., and Karplus, M. 1998. All-atom empirical potential for molecular modeling and dynamics studies of proteins. *J. Phys. Chem. B* **102**: 3586–3616.
- Mandel-Gutfreund, Y., Schueler, O., and Margalit, H. 1995. Comprehensive analysis of hydrogen bonds in regulatory protein DNA-complexes: In search of common principles. *J. Mol. Biol.* **253**: 370–382.
- Mayo, S., Olafson, B., and Goddard, W.I. 1990. DREIDING: A generic force field for molecular simulations. *J. Phys. Chem.* **94**: 8897–8909.
- Menssen, R., Orth, P., Ziegler, A., and Saenger, W. 1999. Decamer-like conformation of a nona-peptide bound to HLA-B\*3501 due to non-standard positioning of the C terminus. *J. Mol. Biol.* **285**: 645–653.
- Mitchell, J.B.O. and Price, S.L. 1990. The nature of the N-H...O=C hydrogen bond: An intermolecular perturbation theory study of the formamide formaldehyde complex. *J. Comput. Chem.* **11**: 1217–1233.
- Mitra, J. and Ramakrishnan, C. 1977. Analysis of O-H...O hydrogen bonds. *Int. J. Pept. Protein Res.* **9**: 27–48.
- Momany, F.A., McGuire, R.F., Burgess, A.W., and Scheraga, H.A. 1975. Energy parameters in polypeptides, VII: Geometric parameters, partial atomic charges, nonbonded interactions, hydrogen bond interactions, and intrinsic torsional potentials for the naturally occurring amino acids. *J. Phys. Chem.* **79**: 2361–2380.
- Morais Cabral, J.H., Jackson, A.P., Smith, C.V., Shikotra, N., Maxwell, A., and Liddington, R.C. 1997. Crystal structure of the breakage-reunion domain of DNA gyrase. *Nature* **388**: 903–906.
- Murray, A.J., Head, J.G., Barjer, J.J., and Brady, R.L. 1998. Tying the knot: Engineering a misfolded form of CD2. *Nat. Struct. Biol.* **5**: 778–782.
- Nemethy, G., Potle, M.S., and Scheraga, H.A. 1983. Energy parameters in polypeptides, 9: Updating of geometric parameters, nonbonded interactions and hydrogen bond interactions for the naturally occurring amino acids. *J. Phys. Chem.* **87**: 1883–1887.
- Nilsson, L. and Karplus, M. 1986. Empirical energy functions for energy minimization and dynamics of nucleic acids. *J. Comput. Chem.* **7**: 591–616.
- Ramakrishnan, C. and Ramachandran, G.N. 1965. Stereochemical criteria for polypeptide and protein chain conformations, II: Allowed conformations for a pair of peptide units. *Biophys. J.* **5**: 909–933.
- Raw, A.S., Coleman, D.E., Gilman, A.G., and Sprang, S.R. 1997. Structural and biochemical characterization of the GTP $\gamma$ S-, GDP-Pi-, and GDP-bound forms of a GTPase-deficient Gly42 $\rightarrow$ Val mutant of Gialpha1. *Biochemistry* **36**: 15660–15669.
- Roberts, V.A., Dauber-Osguthorpe, P., Osguthorpe, D.J., Levin, D.J., and Hagler, A.T. 1986. A comparison of the binding of the ligand trimethoprim to bacterial and vertebrate dihydrofolate reductases. *Israeli J. Chem.* **27**: 198–210.
- Schirmer, T. and Evans, P.R. 1990. Structural basis of the allosteric behavior of phosphofructokinase. *Nature* **343**: 140–145.
- Stickle, D.F., Presta, L.G., Dill, K.A., and Rose, G.D. 1992. Hydrogen bonding in globular proteins. *J. Mol. Biol.* **226**: 1143–1159.
- Tickle, I.J., Laskowski, R.A., and Moss, D.S. 1998a. Error estimates of protein structure coordinates and deviations from standard geometry by full-matrix refinement of  $\gamma$ B- and  $\beta$ B<sub>2</sub>-crystallin. *Acta Cryst. D* **54**: 243–252.
- . 1998b. Rfree and the rfree ratio, I: Derivation of expected values of cross-validation residuals used in macromolecular least-squares refinement. *Acta Cryst. D* **54**: 547–557.
- Vajdos, F.F., Yoo, S., Houseweart, M., Sundquist, W.I., and Hill, C.P. 1997. Crystal structure of cyclophilin A complexed with a binding site peptide from the HIV-1 capsid protein. *Protein Sci.* **6**: 2297–2307.
- Weiner, P.K. and Kollman, P.A. 1981. AMBER: Assisted model building with energy refinement: A general program for model molecules and their interactions. *J. Comput. Chem.* **2**: 287–299.
- Weiner, S.J., Kollman, P.A., Case, D.A., Singh, U.C., Ghio, C., Alagona, G., Profeta, S.J., and Weiner, P. 1984. A new force field for molecular mechanical simulation of nucleic acids and proteins. *J. Am. Chem. Soc.* **106**: 765–784.
- Weiner, S.J., Kollman, P.A., Nguyen, D.T., and Case, D.A. 1986. An all atom field for simulations of proteins and nucleic acids. *J. Comput. Chem.* **7**: 230–252.
- Worthylake, D.K., Wang, H., Yoo, S., Sundquist, W.I., and Hill, C.P. 1999. Structures of the HIV-1 capsid protein dimerization domain at 2.6 Å resolution. *Acta Cryst. D* **55**: 85–92.